

DOI: 10.1002/ange.200602873

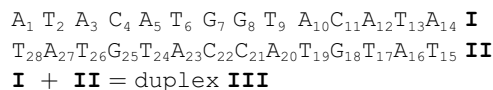
# Diversity in Guanine-Selective DNA Binding Modes for an Organometallic Ruthenium Arene Complex\*\*

Hong-Ke Liu, Susan J. Berners-Price, Fuyi Wang,  
John A. Parkinson, Jingjing Xu, Juraj Bella, and  
Peter J. Sadler\*

Ruthenium(II) arene complexes of the type  $[(\eta^6\text{-arene})\text{Ru}(\text{en})\text{Cl}]^+$  (arene = e.g. *p*-cymene or biphenyl; en = ethylenediamine) can exhibit anticancer activity in vitro and in vivo.<sup>[1]</sup> They are pseudooctahedral, half-sandwich, “piano-stool” complexes with one reactive coordination site (the Ru–Cl bond). Analysis of the distribution of ruthenium in cancer cells in culture<sup>[2]</sup> shows that the level of DNA ruthenation is similar to that of platination by the anticancer drug cisplatin. The binding of cisplatin to DNA gives rise to DNA bending, followed by protein recognition and induction of apoptosis.<sup>[3]</sup> Ruthenium arene complexes are not cross-resistant with cisplatin.<sup>[1]</sup> This may indicate that structural distortions induced in DNA by ruthenium arenes differ significantly from those induced by cisplatin. Calculations<sup>[4]</sup> on adducts of  $\text{Ru}^{\text{II}}$  arene complexes with DNA have suggested that this is the case, but experimental evidence is needed. The extent of DNA ruthenation and the nature of the structural distortions

in DNA appear to correlate with cytotoxic potency,<sup>[5]</sup> and also influence protein recognition.<sup>[6]</sup> The studies reported herein reveal novel and varied modes of interaction of  $[(\eta^6\text{-biphenyl})\text{Ru}(\text{en})\text{Cl}]^+$  (**1**) with duplex DNA.

We chose duplex **III** for study because an NMR analysis has previously been carried out and the kinking induced by GG platination of strand **I** by cisplatin has been characterized.<sup>[7]</sup>



Initially, attempts were made to prepare single strands **I** or **II** that were monoruthenated so that site-specifically ruthenated duplexes could be obtained by addition of the (non-ruthenated) complementary strand.<sup>[8]</sup> Reaction of **1** with the GG strand **I** in a 1:1 molar ratio for 48 h at 310 K gave rise to two monoruthenated products, as separated and identified by HPLC–ESIMS (Figure 1a and Supporting Information).

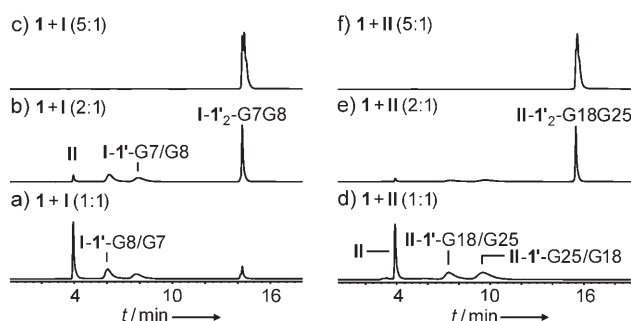


**Figure 1.** HPLC chromatograms for reaction of  $[(\eta^6\text{-biphenyl})\text{Ru}(\text{en})\text{Cl}]\text{PF}_6$  (**1-PF**<sub>6</sub>) with 0.1 mM single-stranded DNA d(ATACATGG-TACATA) (**I**) or d(TATGTACCATGTAT) (**II**) in 100 mM  $\text{NaClO}_4$  at 1/**I** (or **II**) molar ratios of 1:1, 2:1, and 5:1. At a 1/**I** or 1/**II** molar ratio of 5:1, the diruthenated adduct is the only product. **1'** ( $[(\eta^6\text{-biphenyl})\text{Ru}(\text{en})]^{2+}$ ) is bound to GN7. Specific assignments of monoruthenation sites to G7 or G8, and G18 or G25 were not made and hence the four adducts are labeled G7/G8, G8/G7, G18/G25, and G25/G18.

When the molar ratio of **1**:**I** was increased to 2:1 and 5:1, the diruthenated single strand predominated. These data are consistent with selective ruthenation of guanine bases (i.e. G7 and G8) as expected on the basis of competitive mononucleotide reactions.<sup>[9]</sup> Similarly, reactions of **1** with strand **II** gave rise to new HPLC peaks assignable to ruthenation of G18 and G25 (Figure 1d–f and Supporting Information).

For NMR studies, we annealed strand **I** with monoruthenated strand **II**. The fraction corresponding to monoruthenated **II-1'-G18/G25** (Figure 1d) was collected by semipreparative HPLC. This fraction gave a single HPLC peak when it was rechromatographed, which suggests that it was stable. It was annealed with the complementary (nonruthenated) strand **I** by heating to 353 K for 2 min followed by slow cooling to 288 K over 3 h.

We expected that the sample of ruthenated duplex **III** prepared in this way would be ruthenated with  $[(\eta^6\text{-biphenyl})\text{Ru}(\text{en})]^{2+}$  (**1'**) at a single site on strand **II**. However, subsequent analysis of the 2D NOESY NMR data showed

[\*] Dr. H.-K. Liu, Dr. F. Wang, J. Xu, J. Bella, Prof. Dr. P. J. Sadler  
School of Chemistry  
The University of Edinburgh  
King's Buildings  
West Mains Road, Edinburgh EH93JJ (UK)  
Fax: (+44) 131-650-6452  
E-mail: P.J.Sadler@ed.ac.uk

Dr. H.-K. Liu  
School of Chemistry and Environmental Science  
Nanjing Normal University  
Nanjing 210046 (P.R. China)

Prof. Dr. S. J. Berners-Price  
School of Biomedical  
Biomolecular & Chemical Sciences  
The University of Western Australia  
35 Stirling Highway, Crawley WA 6009 (Australia)

Dr. J. A. Parkinson  
WestChem  
Department of Pure and Applied Chemistry  
Thomas Graham Building  
University of Strathclyde  
295 Cathedral Street, Glasgow G1 1XL (UK)

[\*\*] We thank the Wellcome Trust (Travelling Fellowship for H.L. and facilities in the Edinburgh Protein Interaction Centre), the University of Western Australia (Study Leave Grant for S.J.B.-P.), ORS (studentship for J.X.), RC-UK (Rasor), and Oncosense Ltd for support, and colleagues in EC COST Action D20 for stimulating discussions.

Supporting information for this article is available on the WWW under <http://www.angewandte.org> or from the author.

that all four of the guanine residues were ruthenated at N7, and at one of the sites (G18), two different conformers were identified. These adducts are labeled **III-1'-G7**, **III-1'-G8**, **III-1'-G25**, **III-1'-G18i**, and **III-1'-G18n**.

A near-complete assignment of the NOESY NMR spectrum of **III-1'** was achieved for the mixture of five adducts, although the complexity precluded full structural determinations. Assignment was possible because of the known selectivity of **1** for guanines, the localization of structural perturbations to residues close to the ruthenated guanine residue, and the lack of precursor duplex **III** in the HPLC purified sample. Thus, sequential assignments along each strand always led to cross-peaks that were largely identical to those of the nonruthenated duplex. Despite extensive overlap of NOE cross-peaks, little ambiguity in the assignments of individual resonances was found, and cross-validation of signal assignments from related connectivities was possible. The  $^1\text{H}$  NMR chemical shifts of the  $^1\text{H}$  resonances associated with these five adducts are listed in the Supporting Information, and the induced chemical-shift changes are plotted in Figure 2 and the Supporting Information. Structural perturbations induced by ruthenation are clearly localized to within a few ( $\pm 2$ ) base pairs of the ruthenation site in all cases.

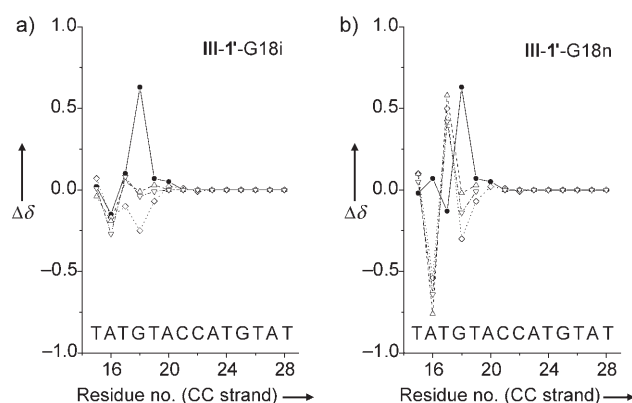
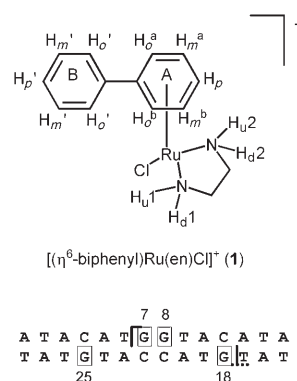


**Figure 2.**  $^1\text{H}$  NMR chemical-shift changes ( $\Delta\delta = \delta(\text{III-1}') - \delta(\text{III})$ ) induced by ruthenation of duplex **III** for resonances of the -CC- strand of a) the **III-1'-G18i** adduct and b) the **III-1'-G18n** adduct. Key: ● aromatic (H6/H8) protons; ◇ H1', △ H2', ▽ H2'' sugar protons.

In the absence of DNA, the amino protons in **1** point towards ( $\text{NH}_u$ ,  $\delta = 6.19$  ppm) or away ( $\text{NH}_d$ ,  $\delta = 4.14$  ppm) from the coordinated arene (Scheme 1).<sup>[10]</sup> On binding to DNA the two amino groups become nonequivalent. A total of ten different pairs of  $\text{NH}_u$  and  $\text{NH}_d$  resonances would therefore be anticipated for the mixture of five different ruthenated adducts. Five distinct  $\text{NH}_u$ - $\text{NH}_d$  cross-peaks were identifiable in the 2D NOESY NMR spectrum at 298 K (see the Supporting Information), thus suggesting that some NH resonances have similar chemical shifts or are not observed for other reasons. The downfield shifts of NH resonances in the adducts are consistent with the presence of H-bonding to



**Scheme 1.** Atom labeling for complex **1** (top) and sites of ruthenation and intercalation on duplex **III** (bottom).

the C6 carbonyl of the coordinated guanine residue.<sup>[10]</sup> Although it was not possible to assign all of the en amino proton resonances, structural information was obtained in specific cases from the observation and interpretation of intramolecular NOEs (see the Supporting Information).

One distinct environment for the noncoordinated phenyl ring B was readily identified from the characteristic pattern of intramolecular NOEs (Supporting Information) and strong shielding of the  $\text{H}_o'$ ,  $\text{H}_m'$ , and  $\text{H}_p'$  protons ( $\Delta\delta \approx -1$  ppm). The NOEs and chemical-shift changes are consistent with intercalation of the arene ring B between DNA bases.<sup>[11]</sup> In the 2D NOESY spectrum at 298 K, only one set of resonances was observed for each of the pairs of *ortho* ( $\text{H}_o'$ ) and *meta* ( $\text{H}_m'$ ) protons, but at 283 K the observation of two slightly different chemical shifts for the  $\text{H}_o'$  cross-peaks provided evidence for slowing of the rotation of the noncoordinated arene in this (intercalated) environment. The assignment of intramolecular NOEs between DNA H1' and arene protons of **1'** revealed that these protons have identical chemical shifts in two of the monoruthenated adducts (**III-1'-G18i** and **III-1'-G7**), which therefore have intercalated arenes in very similar environments.

In three cases, the NMR data were sufficient to allow models to be constructed for the ruthenated adducts on the basis of both observed NOEs and the significant perturbations in chemical shifts of DNA protons with respect to **III** (the nonruthenated duplex). The two adducts ruthenated at G18 are assignable to conformations in which the noncoordinated phenyl ring is either intercalated between G18 and T17 (**III-1'-G18i**; Scheme 1) or nonintercalated (**III-1'-G18n**). The adducts show significant differences in chemical-shift changes for the bases in the sequence T15–G18 (see the Supporting Information and Figure 2). In particular, the A16n and T17n bases of **III-1'-G18n** are significantly distorted, whereas A16i and T17i appear far less perturbed in **III-1'-G18i**.

For **III-1'-G18i**, NOEs between A12 H2 on the complementary strand and the noncoordinated phenyl ring protons, and the strong shielding of the protons of this arene ring ( $\Delta\delta \approx -1$  ppm, see the Supporting Information), in particular, indicate that arene ring B is intercalated between G18 and T17 (Figure 3a). The slight shielding of the T17i  $\text{CH}_3$  protons and deshielding of the T17i  $\text{H}_2'$  and  $\text{H}_2''$  protons (Supporting

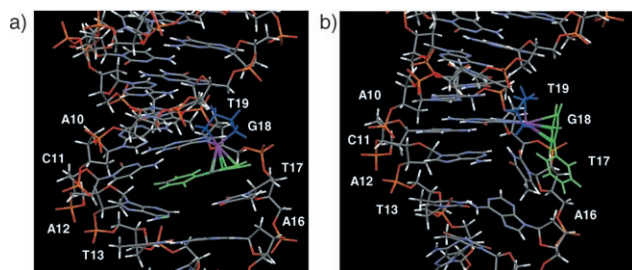


**Figure 3.** Molecular models of two conformers of duplex **III** ruthenated at N7 of G18 with **1'**. a) **III-1'-G18i** showing the intercalation of the arene between G18 and T17. b) **III-1'-G18n** in which the arene is nonintercalated but stacked on a tilted T17. Color code: en blue, biphenyl green.

Information) are consistent with stacking of the Ru-coordinated arene ring A over the T17i aromatic ring and edge-on juxtaposition to the T17i sugar ring.

In contrast, the NOESY and chemical-shift data suggest that the pendant arene in **III-1'-G18n** lies on the surface of the major groove (Figure 3b), thus forcing the T17n base to stack underneath it by tilting, accompanied by a tilt of the A16n base. Such a model explains why the H1' resonances of A16n and T17n are significantly altered with respect to **III** and **III-1'-G18i** and shows how nonintercalation can induce dramatic changes in DNA structure. In the **III-1'-G18i** and **III-1'-G18n** models, the T19 bases are in identical environments, consistent with the NMR data (Supporting Information).

The intramolecular NOEs and strong shielding of the protons of the noncoordinated phenyl ring for the G7 adduct suggest that this ring is intercalated between G7 and T6. The T6 residue appears to be strongly perturbed: no NOESY cross-peaks to either G7 or A5 could be identified and the T6 H2/H2' protons appear to be strongly deshielded (see the Supporting Information).

These studies reveal unique modes of binding of the anticancer complex **1** to duplex DNA. The monofunctional fragment  $\{(\eta^6\text{-biphenyl})\text{Ru}(\text{en})\}^{2+}$  is highly specific for G N7, but mobile at elevated temperature at which migration between guanine residues is facile.<sup>[12]</sup> In contrast, such migration of  $\text{Pt}^{\text{II}}$  am(m)ines is rare. This behavior suggests that organometallic  $\text{Ru}^{\text{II}}$  arene complexes can be readily removed from DNA, which may be beneficial for reversing DNA damage in cells. The specificity of  $\{(\eta^6\text{-biphenyl})\text{-Ru}(\text{en})\}^{2+}$  for guanine is aided by strong H-bonding between an NH of en and C6 carbonyl of G, and by  $\pi$ - $\pi$  stacking involving the noncoordinated phenyl ring of the biphenyl ligand and DNA bases. Such stacking can occur through intercalation between DNA bases (G and T bases in the adducts **III-1'-G7** and **III-1'-G18i**), or with a partially extruded T base, as in **III-1'-G18n**. Arene-base stacking may play a role in determining the rates of reactions of  $\text{Ru}^{\text{II}}$  arene en complexes with DNA, as appears to be the case for mononucleotides.<sup>[9]</sup> Other examples of metal complexes containing DNA-intercalating ligands include  $\text{Ru}^{\text{II}}$ ,  $\text{Rh}^{\text{III}}$ , and di- $\text{Rh}^{\text{II}}$  complexes with phenanthroline derivatives,<sup>[13]</sup> and  $\text{Pt}^{\text{II}}$  complexes with directly bonded or pendant acridine arms.<sup>[14]</sup> It is

well known that DNA structures are relatively flexible. Some intercalators can rotate within intercalation sites.<sup>[15]</sup> Our data suggest that ruthenium arene intercalation is dynamic: equilibria can exist between intercalated (**III-1'-G18i**) and nonintercalated (**III-1'-G18n**) conformers. The present studies provide a structural basis for understanding how the nature of the arene in  $[(\eta^6\text{-arene})\text{Ru}(\text{en})\text{Cl}]^+$  complexes can exert a significant effect on cytotoxicity,<sup>[1]</sup> on excision repair of DNA lesions,<sup>[6]</sup> and on DNA destabilization,<sup>[16]</sup> and provide a basis for future work on sequence-dependent effects of DNA duplex ruthenation.

## Experimental Section

**Ruthenated DNA:** For ruthenation of single strands, microliter aliquots of **1-PF<sub>6</sub>** (10.0 mM) were added to a solution of **I** (17  $\mu\text{L}$ , 1.80 mM),  $\text{NaClO}_4$  (15  $\mu\text{L}$ , 2.0 M), and  $\text{H}_2\text{O}$  (265  $\mu\text{L}$ ), to give 1:1, 2:1, or 5:1 molar ratios of **1/I**, and the mixtures were incubated for 48 h at 310 K in the dark. Similarly, aliquots of **1** were added to **II** (14  $\mu\text{L}$ , 2.13 mM),  $\text{NaClO}_4$  (15  $\mu\text{L}$ , 2.0 M), and  $\text{H}_2\text{O}$  (268  $\mu\text{L}$ ). The ruthenations were monitored by 1D  $^1\text{H}$  NMR spectroscopy, the mixtures separated by HPLC, and the peaks characterized by HPLC-ESIMS.

A similar 1:1 reaction mixture of **1** + **II** (on a 10-mL scale) was separated on a semipreparative C8 ACE-5 column. The fraction eluting at 7.4 min (monoruthenated single-strand fraction **II-1'-G18/G25**, Figure 1d) was collected, freeze-dried, and desalted on a NAP-10 column (Pharmacia Biotech). The sample was then freeze-dried, dissolved in deionized water (200  $\mu\text{L}$ ), and analyzed by HPLC and UV/Vis spectroscopy. Finally,  $\text{NaClO}_4$  (12.5  $\mu\text{L}$ , 2.0 M),  $\text{D}_2\text{O}$  (50  $\mu\text{L}$ ), **I** (140  $\mu\text{L}$ , 1.80 mM), and  $\text{H}_2\text{O}$  (101  $\mu\text{L}$ ) were added to a solution of **II-1'-G18/G25** (196  $\mu\text{L}$ , 1.29 mM) together with dioxane as an internal  $^1\text{H}$  NMR reference. The final concentration of the monoruthenated duplex **III-1'** was 0.51 mM. The resulting DNA solution was annealed by heating briefly from 288 to 353 K for 2 min and cooling slowly to 288 K over 3.5 h. 2D NOESY  $^1\text{H}$  NMR spectra were then recorded at 298 and 283 K.

**Modeling studies:** A structure for duplex d(ATACATGGGTACATA)-d(TATGTACCATGTAT) calculated on the basis of NMR data<sup>[7]</sup> was used to model ruthenated DNA with the biopolymer module of Sybyl (version 6.3, Tripos Inc.). Coordinates from the X-ray crystal structures of **1-PF<sub>6</sub>** (CCDC-170362) allowed accurate incorporation of the Ru complex into the model DNA-Ru construct.

Details of materials used, HPLC, HPLC-ESIMS, NMR, modeling studies, and pH measurements are given in the Supporting Information.

Received: July 18, 2006

Revised: September 7, 2006

Published online: November 22, 2006

**Keywords:** anticancer agents · bioinorganic chemistry · DNA · NMR spectroscopy · ruthenium

[1] Y.-K. Yan, M. Melchart, A. Habtemariam, P. J. Sadler, *Chem. Commun.* **2005**, 4764–4776, and references therein.

[2] F. Wang, B. Zeitlin, P. J. Sadler, D. I. Jodrell, unpublished results.

[3] D. Wang, S. J. Lippard, *Nat. Rev. Drug Discovery* **2005**, *4*, 307–320.

[4] M. C. Colombo, C. Gossens, I. Tavernelli, U. Röthlisberger in *Modelling Molecular Structure and Reactivity in Biological Systems* (Eds.: K. J. Naidoo, M. Hann, J. Gao, M. Field, J. Brady), RSC, Cambridge, **2006**, in press, and references therein.

- [5] F. Wang, A. Habtemariam, E. P. L. van der Geer, R. Fernández, M. Melchart, R. J. Deeth, R. Aird, S. Guichard, F. P. A. Fabbiani, P. Lozano-Casal, I. D. H. Oswald, D. I. Jodrell, S. Parsons, P. J. Sadler, *Proc. Natl. Acad. Sci. USA* **2005**, *102*, 18269–18274.
- [6] O. Novakova, J. Kasparkova, V. Bursova, C. Hofr, M. Vojtkova, H. Chen, P. J. Sadler, V. Brabec, *Chem. Biol.* **2005**, *12*, 121–129.
- [7] J. A. Parkinson, Y. Chen, P. del S. Murdoch, Z. Guo, S. J. Berners-Price, T. A. Brown, P. J. Sadler, *Chem. Eur. J.* **2000**, *6*, 3636–3644.
- [8] HPLC showed that all four G residues in **III** are readily ruthenated at 310 K; see the Supporting Information.
- [9] H. Chen, J. A. Parkinson, R. E. Morris, P. J. Sadler, *J. Am. Chem. Soc.* **2003**, *125*, 173–186.
- [10] H. Chen, J. A. Parkinson, S. Parsons, R. A. Coxall, R. O. Gould, P. J. Sadler, *J. Am. Chem. Soc.* **2002**, *124*, 3064–3082.
- [11] Recently we studied ruthenation of the 6mer d(CGGCCG)<sub>2</sub>: H. Liu, F. Wang, J. A. Parkinson, J. Bella, P. J. Sadler, *Chem. Eur. J.* **2006**, *12*, 6151–6165. The NMR data suggested that arene intercalation can occur, but were not sufficient to allow models of the interactions to be constructed.
- [12] HPLC studies of similar adducts of the related complex [(η<sup>6</sup>-p-cymene)Ru(en)Cl]<sup>+</sup> with duplex **III** show that such migration is very slow at ambient temperature.
- [13] a) K. E. Erkkila, D. T. Odom, J. K. Barton, *Chem. Rev.* **1999**, *99*, 2777–2795; b) L. M. Wilhelmsson, F. Westerlund, P. Lincoln, B. Norden, *J. Am. Chem. Soc.* **2002**, *124*, 12092–12093; c) A. Greguric, I. D. Greguric, T. W. Hambley, J. R. Aldrich-Wright, J. G. Collins, *J. Chem. Soc. Dalton Trans.* **2002**, 849–855.
- [14] a) B. E. Bowler, S. J. Lippard, *Biochemistry* **1986**, *25*, 3031–3038; b) W. I. Sundquist, D. P. Bancroft, S. J. Lippard, *J. Am. Chem. Soc.* **1990**, *112*, 1590–1596; c) E. Ceci, R. Cini, A. Karaulov, M. B. Hursthouse, L. Maresca, G. Natile, *J. Chem. Soc. Dalton Trans.* **1993**, 2491–2497; d) J. R. Choudhury, U. Bierbach, *Nucleic Acids Res.* **2005**, *33*, 5622–5632.
- [15] J. Gallego, *Nucleic Acids Res.* **2004**, *32*, 3607–3614.
- [16] O. Novakova, H. Chen, O. Vrana, A. Rodger, P. J. Sadler, V. Brabec, *Biochemistry* **2003**, *42*, 11544–11554.
-